Am J Physiol Gastrointest Liver Physiol 302: G1253–G1263, 2012.
First published March 29, 2012; doi:10.1152/ajpgi.00329.2011.

The transcription factor HNF-4α: a key factor of the intestinal uptake of fatty acids in mouse

Vincent Frochot,[1,2,3] Malik Alqub,[1,2,3] Anne-Laure Cattin,[1,2,3] Véronique Carrière,[1,2,3] Anne Houllier,[1,2,3] Floriane Baraille,[1,2,3] Laurence Barbot,[4] Susan Saint-Just,[1,2,3] Agnès Ribeiro,[1,2,3] Michel Lacasa,[1,2,3] Philippe Cardot,[1,2,3] Jean Chambaz,[1,2,3] Monique Rousset,[1,2,3] and Jean-Marc Lacorte[1,2,3]

[1]*Centre de Recherche des Cordeliers, Université Pierre et Marie Curie, UMRS 872, Paris, France;* [2]*Institut National de la Santé et de la Recherche Médicale, U872, Paris, France;* [3]*Université Paris Descartes, UMRS 872, Paris, France;* [4]*Laboratoire de Coprologie, AP-HP, Groupe Hospitalier Pitié-Salpêtrière, Paris, France*

Submitted 18 August 2011; accepted in final form 25 March 2012

Frochot V, Alqub M, Cattin A, Carrière V, Houllier A, Baraille F, Barbot L, Saint-Just S, Ribeiro A, Lacasa M, Cardot P, Chambaz J, Rousset M, Lacorte J. The transcription factor HNF-4α: a key factor of the intestinal uptake of fatty acids in mouse. *Am J Physiol Gastrointest Liver Physiol* 302: G1253–G1263, 2012. First published March 29, 2012; doi:10.1152/ajpgi.00329.2011.—With an excessive postprandial accumulation of intestine-derived, triglyceride-rich lipoproteins being a risk factor of cardiovascular diseases, it is essential to characterize the mechanisms controlling the intestinal absorption of dietary lipids. Our aim was to investigate the role of the transcription factor hepatocyte nuclear factor (HNF)-4α in this process. We used transgenic mice with a specific and inducible intestinal knockout of Hnf-4α gene. One hour after a lipid bolus, in the presence of the lipase inhibitor tyloxapol, lower amounts of triglycerides were found in both plasma and intestinal epithelium of the intestine-specific Hnf-4α knockout (Hnf-4α$^{int\Delta}$) mice compared with the Hnf-4α$^{loxP/loxP}$ control mice. These discrepancies were due to a net decrease of the intestinal uptake of fatty acid in Hnf-4α$^{int\Delta}$ mice compared with Hnf-4α$^{loxP/loxP}$ mice, as assessed by the amount of radioactivity that was recovered in intestine and plasma after gavage with labeled triolein or oleic acid, or in intestinal epithelial cells isolated from jejunum after a supply of labeled oleic acid-containing micelles. This decreased fatty acid uptake was associated with significant lower levels of the fatty acid transport protein-4 mRNA and protein along the intestinal tract and with a lower acyl-CoA synthetase activity in Hnf-4α$^{int\Delta}$ mice compared with the control mice. We conclude that the transcription factor HNF-4α is a key factor of the intestinal absorption of dietary lipids, which controls this process as early as in the initial step of fatty acid uptake by enterocytes.

enterocytes; Hnf-4α knockout; dietary fat; fatty acid transport protein-4

INTESTINE, THE FIRST ORGAN facing digestion products, contributes to energy homeostasis through the absorption, metabolism, and transfer of nutrients to the organism. It is now established that an excessive postprandial accumulation in plasma of triglyceride-rich lipoproteins (TRL) originating from intestine is a risk factor of cardiovascular diseases (2, 4, 20, 21, 31).

Enterocytes, the polarized absorptive cells of the intestinal epithelium, ensure the transfer of dietary lipids to the organism through complex processes (for reviews, Refs. 28, 47). In the intestinal lumen, triglycerides (TG), the major components of dietary lipids, are hydrolyzed mainly by pancreatic enzymes into fatty acids and monoglycerides, which are associated with biliary secretions to form lipid micelles, allowing their absorption by enterocytes (for reviews, Refs. 32, 39). The uptake of fatty acids occurs by passive diffusion and by a saturable/protein-mediated mechanism comprising the fatty acid translocase (FAT/CD36), the fatty acid-binding protein (FABP) from the plasma membrane (FABPpm), as well as the fatty acid transport protein (FATP) family (13, 30, 43). After resynthesis within the endoplasmic reticulum (ER) membrane, TG are used to form chylomicrons (CM), the intestine-specific postprandial form of TRL, which will be secreted into the lymph and then directed toward circulation. The assembly of one TRL results from the fusion between one apolipoprotein B (apoB) molecule, which is necessary for their formation (8), and one independently formed TG droplet. The microsomal TG transfer protein (MTP) has a prominent role in CM assembly, ensuring the lipidation-dependent stabilization of apoB and the transfer of lipids to the TG droplet in the ER lumen (for review, Ref. 18). TRL thus comprises a neutral lipid core (essentially TG), surrounded by a monolayer of amphipatic lipids and apolipoproteins, particularly the structural apoB and the exchangeable apolipoproteins A-I (apoA-I), E (apoE), and A-IV (apoA-IV). During the postprandial period, TG are also transiently stored in enterocytes, as cytosolic lipid droplets, which can be subsequently hydrolyzed to reenter the secretory pathway (37). Many genes are involved in the control of TG secretion and storage. Thus perturbations of their basal level of expression and/or their nutrient-dependent modulation should interfere with the enterocyte function of dietary lipid absorption.

The transcription factor hepatocyte nuclear factor (HNF)-4α, which belongs to the superfamily of nuclear receptors, is expressed in liver, pancreas, kidney, and intestine (10, 27, 42). Conditional invalidation of the Hnf-4α gene in adult mouse liver underlined the key role of HNF-4α in the control of genes involved in lipid metabolism in this organ (17). Despite its strong intestinal expression, the function of HNF-4α is much less documented in intestine than in liver (for review, Ref. 36). Our laboratory previously demonstrated that, in mice and in Caco-2/TC7 enterocytes, HNF-4α is involved in the transcriptional activation of apoA-IV by dietary lipid-containing postprandial micelles (6), and, through a large transcriptome analysis, we showed that postprandial micelles modulate specifically the expression of 47 genes related to three main function categories, namely cell adhesion/architecture, cell signaling, and glucose/lipid metabolism, in enterocytes. Among these 47 genes, 20 genes, including apoA-IV, apoB, and MTP, had putative or known binding sites for HNF-4α (3). Moreover,

Address for reprint requests and other correspondence: M. Rousset, UMRS 872-Team 4, 15 rue de l'école de medicine, 75006 Paris, France (e-mail: monique.rousset@crc.jussieu.fr).

through a transcriptome and metabolome analysis, Stegmann et al. (44) suggested that HNF-4α could play a major role in lipid metabolism in differentiated enterocytes.

Using a transgenic mouse model allowing an inducible and intestine-specific knockout (KO) of the Hnf-4α gene, our laboratory previously showed that HNF-4α controls intestinal epithelium homeostasis and cell architecture (7). In the present study, we aimed to determine whether and how HNF-4α could be involved in the intestinal transfer of TG. Our results demonstrate that this transcription factor plays a key role in the postprandial secretion and storage of TG. These effects rely on an impaired uptake of fatty acids in the absence of intestinal HNF-4α, which was associated with a downregulation of the expression of FATP4 and a decreased acyl-CoA synthetase (ACS) activity.

MATERIAL AND METHODS

Animals and treatments. The procedure for obtaining Hnf-4α$^{int\Delta}$ mice ("int" standing for intestinal, and "Δ" for deletion) was described in Cattin et al. (7). Hnf-4α$^{loxP/loxP}$ mice (17) and Villin-CreERT2 mice (11), from the same C57Bl6 background, were mated to obtain Hnf-4α$^{loxP/loxP}$/villin-CreERT2 mice for a tamoxifen-inducible and intestine-specific KO of the Hnf-4α gene. The Cre recombinase activity in epithelial cells of intestine was induced by a daily gavage with tamoxifen (1 mg/100 μl, Sigma-Aldrich), in 5% carboxymethylcellulose, for 5 days. For experiments, 12-wk-old male mice were used. Both control Hnf-4α$^{loxP/loxP}$ and Hnf-4α$^{loxP/loxP}$/villin-CreERT2 mice received tamoxifen treatment. A net decrease of HNF-4α expression, down to 20% of the control value, was observed in the jejunum of Hnf-4α$^{int\Delta}$ compared with Hnf-4α$^{loxP/loxP}$ mice (7). Due to the potential interference of tamoxifen with lipid metabolism (12, 24), analyses were performed 3 wk after the treatment with tamoxifen, as already reported for the intestine-specific KO of MTP (48). All experiments were performed 4 h after food withdrawal. Then mice received or not an intraperitoneal injection of 1 mg Tyloxapol WR-1339 (Sigma-Aldrich) per gram of body weight and were force fed 30 min later with 150 μl of olive oil. For fatty acid uptake experiments, 20 μl of [1-^{14}C]oleic acid (OA; 2 μCi, specific activity 50 μCi/μmol) or of [carboxyl-^{14}C]triolein (2 μCi, 80–120 μCi/μmol) (Perkin-Elmer) were added to the lipid bolus.

Experimental procedures conformed to the French guidelines for animal studies from the regional Animal Care and Use Committee (CREEA Ile de France No. 3, agreement number p3/2008/46), which approved this study.

Plasma parameters. After anesthesia, blood was collected from inferior vena cava into EDTA-containing tubes. Cholesterol, glycerol, and TG were measured with kits from Diasys France (Condom).

Isolation of intestinal epithelial cells. After euthanasia, the small intestine was excised, flushed with PBS, and divided into three equal fragments (~10 cm each) from the beginning of jejunum to the end of ileum [I1 (jejunum), I2 (jejunum and ileum), and I3 (ileum)]. The first centimeter of I1 was used for histology (see below).

To isolate the epithelial cells, the rest of the intestinal fragments were cut into small pieces and incubated overnight, at 4°C, in 3 ml of cell recovery solution (BD Biosciences) (1) containing 2% protease inhibitor cocktail (Sigma-Aldrich). The epithelial cell homogenate was filtered, washed with PBS, centrifuged to obtain villus epithelial cells, and then homogenized for protein extraction for Western blot and enzyme (MTP, ACS) activity analyses and for intestinal TG measurements.

For fatty acid uptake experiments, 100 μl of suspended epithelial cells (corresponding to 30–100 μg of proteins) isolated freshly from jejunum fragments were centrifuged, and the cell pellet was incubated at 37°C with 100 μl of micelles (OA 0.6 mM, lysophosphatidylcholin 0.2 mM, cholesterol 0.05 mM, monoacylglycerol 0.2 mM) (6), which contained [1-^{14}C]oleate (0.2 μCi/4 nmol in 100 μl of micelles). Reactions were stopped at different times by the addition of 10 volumes (1 ml) of cold PBS before centrifugation. The cell pellet was washed three times in cold PBS and lysed (100 μl 1% Triton X-100 and 5 mM EDTA, in PBS) before addition of 3 ml of scintillation liquid and counting in a Perkin-Elmer counter.

Tissue isolation and histology. One centimeter of jejunum fragment (I1) was immediately embedded in tissue-tek (Shandon) and stored at −80°C until use for lipid analysis or fixed overnight at 4°C in alcohol-formalin acetic acid before being embedded in paraffin for immunofluorescence studies. The primary antibodies used were goat anti-CD36 (AF 2519 R&D systems) and rabbit anti-FATP4 (Abnova) antibodies. The secondary antibodies were Alexafluor-conjugated donkey anti-goat or anti-rabbit 546 (Molecular Probes). Nuclear counterstaining was performed with 4,6-diamidino-2-phenylindole. For histological lipid analysis, cryostat sections (10–15 μm) were applied onto gelatin-coated glass slides, fixed in paraformaldehyde solution (4%) for 30 min, and then used for staining with oil red O and hematoxylin. Immunofluorescence or lipid staining was examined by epifluorescence microscopy (Axiophot microscope connected to an Axiocam camera using the Axiovision 4.5 software; Carl Zeiss).

Separations of lipoproteins. Lipoproteins were separated by fast protein liquid chromatography (FPLC), using two superose 6 (10/300 GL ref 17–5172-01, GE Healthcare) columns operating in series. Plasma from each mouse, collected 1 h after gavage, was injected (200 μl of plasma) and eluted at a constant flow rate of 0.4 ml/min with NaCl (150 mM), EDTA (0.3 mM), and sodium azide (0.04%)-containing Tris buffer (pH 7.4). Fractions of 200 μl were collected and assayed for cholesterol and TG.

Analysis of lipids. Epithelial cell lysates isolated from mouse jejunum, 1 h after a bolus of olive oil containing radiolabeled OA or triolein, were extracted with five volumes of chloroform-methanol (2:1 vol/vol), with vigorous shaking for 10 min. After centrifugation for 20 min at 1,000 *g*, the lower organic phase was collected and dried. Lipids were dissolved in 200 μl of chloroform-methanol. An aliquot (75 μl) was taken for liquid scintillation counting (Perkin Elmer counter), and another (75 μl) was used for silica gel thin-layer chromatography in hexane-diethyl ether-acetic acid (80:20:2). The lipids were stained with iodine, and the different bands were excised and counted.

For the analysis of lipids in feces, four mice of each group were placed in metabolic cages for 2 days under a high-fat diet enriched in lard (lipids accounting for 55% of calories with 40% from OA). Weight and food consumption were monitored. For lipid analysis, 200 mg of feces were diluted in chloroform/methanol (2:1 vol/vol) and homogenized. After decantation, 10 μl of supernatant were used for silica gel thin layer chromatography in hexane-diethyl ether-formic acid (80:20:2) along with standards for cholesterol, OA, and mono-, di-, and trioleylglycerol. The spots were revealed by phosphomolybdic acid in ethanol (20 g/100 ml) for densitometric quantification of lipids in the feces samples (Image-Quant, LAS 4000, GE Healthcare).

Western blot analysis. Intestinal epithelial cells were treated with lysis buffer containing 5% protease inhibitor cocktail (Sigma-Aldrich), 1% Triton X-100, and 5 mM EDTA, in PBS. Forty micrograms of total proteins or 2 μl of plasma (containing protease inhibitor cocktail) were loaded on 2% SDS-PAGE gels for apoB and albumin detections or 12% SDS-PAGE gels for MTP, adipose differentiation-related protein (ADRP), tail-interacting protein 47 (TIP47), CD36, FATP4, I-FABP, and L-FABP, and α-actin detections. Primary antibodies that were used are goat anti-apoB and mouse monoclonal anti α-actin (Chemicon), mouse monoclonal anti-MTP (BD Biosciences), rabbit anti-FATP4, goat anti-albumin and mouse monoclonal anti-L-FABP (Abcam), rabbit monoclonal anti-I-FABP (Epitomics), goat anti-mouse CD36 (AF2519) and rat monoclonal anti-ADRP (R&D systems), and guinea pig anti-TIP47 (Progen) antibodies. Secondary peroxidase-conjugated antibodies were horse anti-goat IgG (Vector Laboratories, AbCys), sheep anti-mouse IgG, donkey anti-rabbit IgG

and goat anti-rat IgG (Amersham), and rabbit anti-guinea pig IgG (DakoCytomation) antibodies. The blots were developed with ECL Western blotting reagents, according to the manufacturer's instructions (Amersham). Films were scanned, and signals were quantified by using Image-Quant software (Molecular Dynamics).

MTP activity assay. Intestinal epithelial cells were homogenized in a buffer containing 10 mM Tris·HCl (pH 7.4), 150 mM NaCl, 1 mM EDTA, and 2% protease inhibitor cocktail (Sigma-Aldrich). MTP activity was measured with an MTP assay kit (Roar Biomedical) by incubating, for different times at 37°C, 100 μg of proteins of intestinal epithelium homogenates with 4 μl of donor solution and 4 μl of acceptor solution (according to manufacturer's instructions) in homogenization buffer (total volume 200 μl). Fluorescence was measured (485-nm excitation wavelength and 538-nm emission wavelength) at 37°C every 15 min for 115 min using the Fluostar Ascent FL (Labsystems).

ACS assays. ACS activity assay, adapted from Hall et al. (15), measured the conversion of [1-^{14}C]oleate (C18:1, 0.01 μCi/assay) to [1-^{14}C]oleyl-CoA or of [1-^{14}C]hexacosanoic acid (Isobio, Fleurus, Belgium) (C26:0, 0.01 μCi/assay) to [1-^{14}C]hexacosanoyl-CoA. Each assay was performed with lysates of epithelial cells isolated from the jejunum (I1) fragment (50 μg of proteins), in 250 μl of 100 mM Tris·HCl, pH 7.5, buffer containing 5 mM $MgCl_2$, 2% Triton X-100 (final 0.4%), 20 μM [1-^{14}C]oleate or [1-^{14}C]hexacosanoic acid, 10 mM ATP, 200 μM dithiothreitol, and 200 μM CoASH. The reactions were stopped after 1, 2, or 5 min by the addition of 1.25 ml of isopropanol-heptane-H_2SO_4 (40:10:1 vol/vol/vol), 0.5 ml of H_2O, and 0.75 ml of heptane to facilitate organic phase separation. The aqueous phase was treated three times with 0.75 ml of heptane to remove unreacted fatty acids, and the radioactivity was determined by liquid phase scintillation counting in a Perkin-Elmer counter. The initial reaction rate (V0), corresponding to the slope of the initial linear part of the curves, was expressed as micromoles per minute per milligram of protein.

RNA extraction and gene expression analysis. Total RNA was isolated from epithelial cells of jejunum by Tri-reagent solution (MRC). Reverse transcription was performed with 1 μg RNA in 20 μl reaction buffer. Semiquantitative real-time polymerase chain reaction was performed using the Light Cycler System with SYBR Green, according to the manufacturer's procedures (Roche Molecular Biochemicals). Primer sequences used for each mRNA were designed by Universal Probe Library Assay Design Center (Roche, Meylan) and are reported in Table 1. Primers were synthesized by MWG-Biotech (Paris). Results are expressed as the ratio between the mRNA of interest and L19 mRNA.

Statistical analysis. Statistical analyses were performed with nonparametric Mann-Whitney test. Results are expressed as means ± SE.

RESULTS

The intestinal postprandial secretion of TRL is impaired in Hnf-4α$^{int\Delta}$ mice. Postprandial plasma TG content was compared between Hnf-4α$^{loxP/loxP}$ and Hnf-4α$^{int\Delta}$ mice, 4 h after food withdrawal (T0) and after a lipid bolus, without or with a pretreatment with tyloxapol, which inhibits the remodeling of intestinal TRL by lipoprotein lipase in plasma (5) (Fig. 1*A*). No difference in the plasma TG content was observed at T0 between both groups of mice (Fig. 1*B*). Without tyloxapol, a peak of plasma TG occurred 1 h after the bolus of olive oil in Hnf-4α$^{loxP/loxP}$ mice (from 0.43 ± 0.05 mmol/l at T0 to 0.75 ± 0.04 mmol/l at 60 min; $P < 0.001$) (Fig. 1*B*). By contrast, no significant peak of plasma TG was observed in Hnf-4α$^{int\Delta}$ mice (0.48 ± 0.02 mmol/l at T0 and 0.55 ± 0.05 mmol/l at 60 min), even 6 or 12 h after the lipid bolus (Fig. 1*B*). After a treatment with tyloxapol, the amount of plasma TG regularly increased over a period of 2 h after the lipid bolus in Hnf-4α$^{loxP/loxP}$ mice, as expected (Fig. 1*C*, *top*), reaching 2.5 times the basal value 1 h after the lipid bolus (0.44 ± 0.02 to 1.11 ± 0.03 mmol/l; $P < 0.001$). Here again, no obvious increment of plasma TG was observed in Hnf-4α$^{int\Delta}$ mice (0.55 ± 0.05 and 0.64 ± 0.02 mmol/l).

Plasma TG and cholesterol elution profiles were further analyzed by FPLC, 1 h after the lipid bolus, in mice treated with tyloxapol (Fig. 2*A*). Cholesterol amount was similar in both intestine-specific Hnf-4α KO mice and control mice (0.92 ± 0.14 and 0.90 ± 0.03 mmol/l, respectively; Fig. 2*A*, *middle*), even though the size of HDL, to which cholesterol was associated, appeared more heterogeneous in Hnf-4α$^{int\Delta}$ (fractions 85–105) than in Hnf-4α$^{loxP/loxP}$ mice (fractions 90–100) (Fig. 2*A*, *left*). By contrast, TG levels in the very-low-density lipoprotein/CM fractions were significantly lower in Hnf-4α$^{int\Delta}$ (0.66 ± 0.02 mmol/l) compared with Hnf-4α$^{loxP/loxP}$ mice (1.15 ± 0.02 mmol/l) (Fig. 2*A*, *right*), suggesting a decreased lipidation and/or number of secreted TRL. The concomitant and specific lower level of apoB48 (0.64 ± 0.04 in control and 0.32 ± 0.07 in Hnf-4α$^{int\Delta}$ mice; $P < 0.01$) (Fig. 2*B*, plasma), without difference in the amount of the liver-specific apoB100 (0.28 ± 0.01 and 0.27 ± 0.07), suggested that the number of lipoprotein molecules secreted by intestine was lower in Hnf-4α$^{int\Delta}$ mice. However, with apoB48 being produced also by liver in mouse, its intestine-specific part was evaluated by analysis in the purified intestinal epithelial cells. The intestinal apoB48 protein level of Hnf-4α$^{int\Delta}$ mice (0.68 ± 0.06) represented only 59% of the amount present in control mice (1.15 ± 0.11) (Fig. 2*B*, intestinal epithelial cells). Because MTP is expressed under the control of HNF-4α and is necessary for apoB and TG droplet lipidation within the ER lumen before their association for secretion, we quantified its amount and activity in intestinal epithelial cells. The MTP protein amount was found similar in both mouse groups at T0. One hour after the lipid bolus, the level of MTP protein significantly increased in Hnf-4α$^{loxP/loxP}$, but remained unchanged in Hnf-4α$^{int\Delta}$ (1.45 ± 0.15 and 1.07 ± 0.05, respectively, at 60 min; $P < 0.01$) (Fig. 2*C*, *left* and *middle*). Accordingly, the MTP activity was lower in Hnf-4α$^{int\Delta}$ than in control mice 60 min after lipid bolus (2.2 ± 0.2 and 3.1 ± 0.1 $mF{\cdot}U^{-1}{\cdot}min^{-1}{\cdot}\mu g\ protein^{-1}$, respectively; $P < 0.01$) (Fig. 2*C*, *right*).

Newly synthesized TGs are not retained in the intestinal epithelium of Hnf-4α$^{int\Delta}$ mice. To determine whether the decreased amount of plasma TG was due to the retention of the newly synthesized TG (packaged in the core of CM or stored in cytosolic lipid droplets) in enterocytes of Hnf-4α$^{int\Delta}$ mice, the presence of TG was analyzed in the jejunum of Hnf-4α$^{int\Delta}$ and Hnf-4α$^{loxP/loxP}$ mice before and 1 h after the lipid bolus.

Table 1. *Sequence of primers for semiquantitative RT-PCR*

Gene	Sense Primer 5′ → 3′	Antisense Primer 5′ → 3′
ACSL1	GCAAGAACAGCTGAAGCCC	AGGTGCCATTTGGCAGCCA
ACSL3	CAATTACAGAAGTGTGGGACT	CACCTTCCTCCCAGTTCTTT
ACSL5	GGCCAAACAGAATGCACAG	GGAGTCCCAACATGACCTG
ADRP	GCCAGGAAGAATGTGTATAG	CAGATCGCTGGGTCTC
CD36	GAGCCATCTTTGAGCCTTCA	TCAGATCCGAACACAGCGTA
FABPpm	ATGGCTGCTGCCTTTCAC	GATCTGGAGGTCCCATTTCA
FATP4	TATGGCTTCCCTGGTGTACTAA	TTCTTCCGGATCACCACAGTC
TIP47	GAGGGCTGGACAGACTGC	GTTCCTTAGTATCCGCCAAAAC
L19	ATGTATCACAGCCTGTACCTG	CGTGCTTCCTTGGTCTTAGAC

See text for definition of genes.

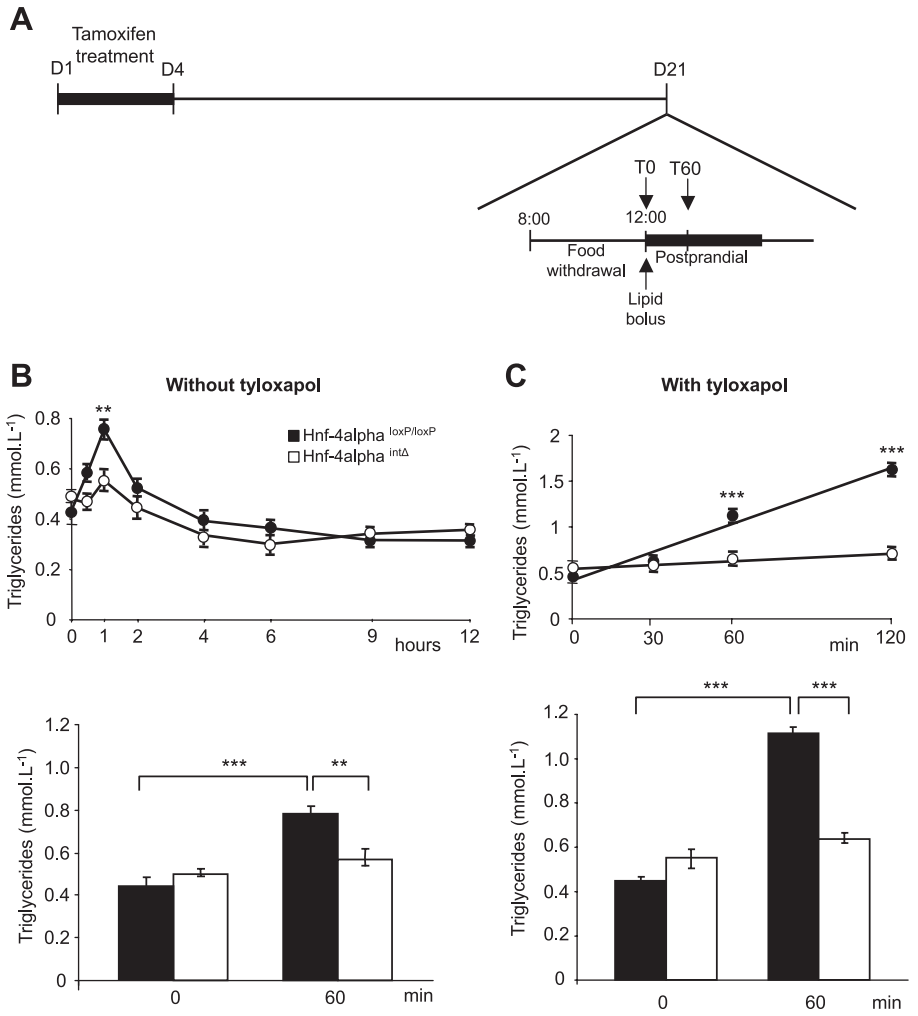

Fig. 1. *A*: a schematic representation of the mouse treatments is presented. Plasma triglycerides (TG) concentrations were measured 4 h after food withdrawal (T0) and after a lipid bolus without (*B*) or with (*C*) a pretreatment with tyloxapol (30 min before the administration of olive oil bolus). *Top* panels correspond to a representative curve obtained over 12 h (*B*) or 2 h (*C*) after the lipid bolus. Note the absence of decrease of plasma TG between 1 h and 2 h after the lipid bolus in tyloxapol-treated mice. *Bottom* panels correspond to the values obtained 4 h after food withdrawal (0) and 60 min after the lipid bolus (solid symbols or bars, Hnf-4α$^{loxP/loxP}$ mice; open symbols or bars, Hnf-4α$^{int\Delta}$ mice; $n = 4$ for each group and in each condition). D, day. Values are means ± SE. $^{**}P < 0.01$, $^{***}P < 0.001$.

The amount of TG was similar in KO mice and control mice at T0 (0.06 ± 0.01 and 0.07 ± 0.01 mmol/g protein, respectively), but was four times lower in Hnf-4α$^{int\Delta}$ (0.21 ± 0.04 mmol/g protein) than in the control mice (0.83 ± 0.09 mmol/g protein; $P < 0.001$) 1 h after the lipid bolus (Fig. 3*A*). The size of the lipid droplets observed in intestinal epithelium corresponding most probably to cytosolic lipid droplets, we analyzed the amounts of ADRP (perilipin 2/ADFP) and TIP47 (perilipin 3), which are the two members of perilipin-adipophilin-TIP47 family proteins associated with cytosolic lipid droplets in enterocytes (22). The amount of ADRP or TIP47 proteins was similar in both groups of mice before the lipid bolus (Fig. 3, *C* and *E*). One hour after the lipid bolus, the difference in TIP47 protein amounts between Hnf-4α$^{int\Delta}$ and control mice did not reach significance, but interindividual variations were observed in each group. By contrast, the level of ADRP protein greatly increased in Hnf-4α$^{loxP/loxP}$ mice, but remained unchanged in Hnf-4α$^{int\Delta}$ mice (0.84 ± 0.05 and 0.17 ± 0.04, respectively; $P < 0.001$) (Fig. 3*B*). No significant difference in the levels of ADRP mRNA was observed neither 1 h after the lipid bolus, nor between the two groups of mice (Fig. 3*B*), indicating that the specific and significant increase of ADRP protein level after the lipid bolus in control mice was most probably the consequence of a rapid posttranslational, lipid-dependent stabilization of the protein, as reported in hepatocytes (14). The level of TIP47 mRNA increased 1 h after the lipid bolus in Hnf-4α$^{loxP/loxP}$ mice, but remained unchanged in Hnf-4α$^{int\Delta}$ mice, tending to be at a slightly higher level than in control mice at T0 (Fig. 3*D*).

The uptake of fatty acids is decreased in Hnf-4α$^{int\Delta}$ mice. The lower amounts of TG in the intestinal epithelium and the plasma of Hnf-4α$^{int\Delta}$ mice suggested an impairment of the fatty acid uptake by enterocytes. Since this could result from an impairment of the digestion process of alimentary TG, the uptake of OA was compared in the two groups of mice after a lipid bolus containing radiolabeled triolein or OA. We observed significant lower amounts of the radioactivity recovered from radiolabeled triolein or OA, in both intestinal epithelium and plasma of Hnf-4α$^{int\Delta}$ mice compared with control mice, 1 h after the lipid bolus (Fig. 4*A*). However, in Hnf-4α$^{int\Delta}$ mice, the same results were obtained with triolein and OA, in intestinal epithelium or plasma (Fig. 4*A*), suggesting that the decreased fatty acid uptake in these mice was not due to a decreased activity of the luminal lipase. Finally, there was no difference in the intraepithelial repartition of labeling within free fatty acids (FFA, 1%) and newly synthesized phospholipids/monooleylglycerol (3%), diacylglycerol (DG, 6%), and TG (90%) between intestine-specific Hnf-4α KO mice and control mice (Fig. 4*B*), demonstrating that the uptake of fatty acid was impaired, but not the capacity of Hnf-4α$^{int\Delta}$ enterocytes to

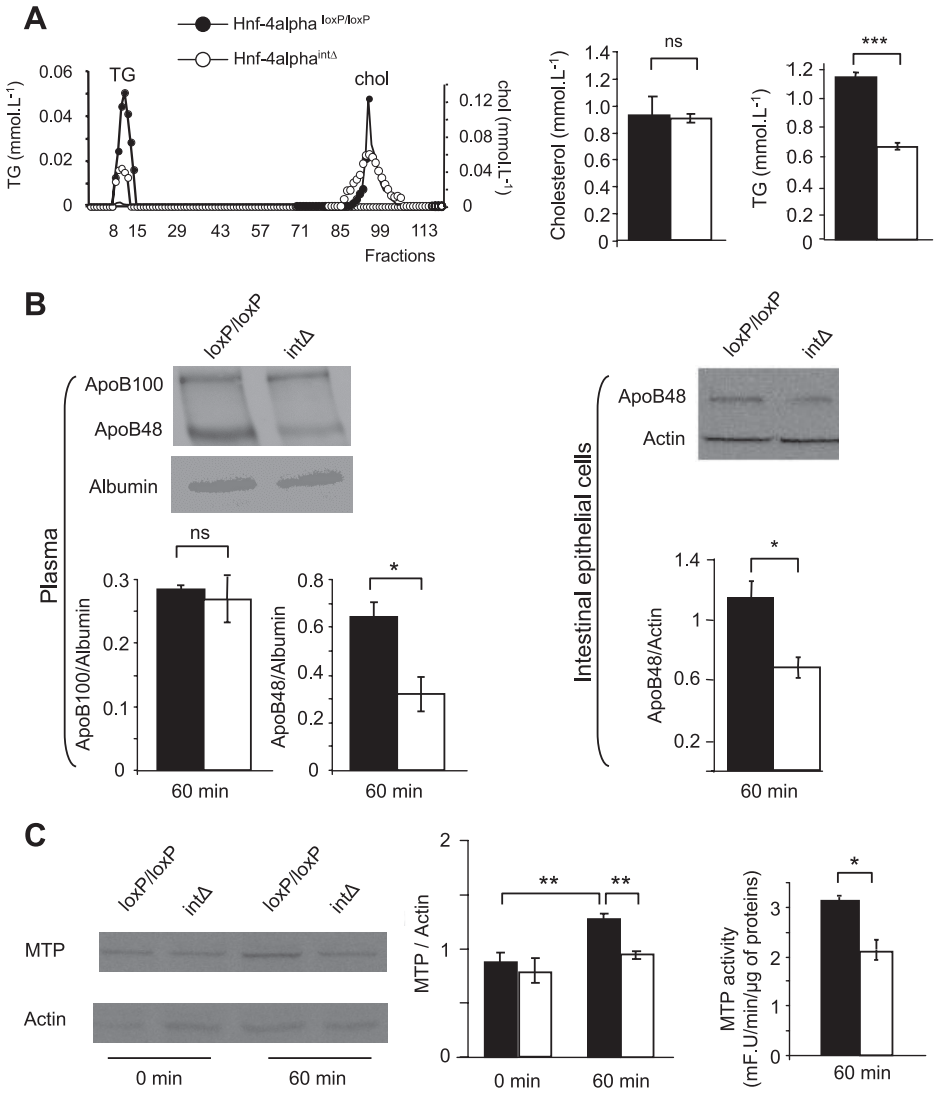

Fig. 2. *A*: postprandial plasma TG and cholesterol were analyzed by fast protein liquid chromatography (FPLC), 1 h after the lipid bolus, in mice treated with tyloxapol. Representative FPLC results are shown on the *left*. Total plasma TG and cholesterol are reported on the *right* (solid symbols or bars, Hnf-4α$^{loxP/loxP}$ mice; open symbols or bars, Hnf-4α$^{int\Delta}$ mice; $n = 4$ for each group of mice). *B*: apolipoprotein (Apo) B100 and apoB48 protein levels were analyzed 1 h after the lipid bolus, by Western blot, in plasma (*left*, representative Western blots) or in the intestinal epithelial cells (*right*, representative Western blots), and normalized by the signal obtained for albumin or actin (*bottom* panels). *C*: microsomal TG transfer protein (MTP) protein level was analyzed by Western blot (*left*, representative Western blots) and normalized by the signal obtained for actin (*middle*). MTP activity was measured 1 h after the lipid bolus (*right*) ($n = 4$ for each group in each experiment). Values are means ± SE. ns, Not significant. $^*P < 0.05$, $^{**}P < 0.01$, $^{***}P < 0.001$.

resynthesize TG from fatty acid. A significant lower uptake of fatty acids was observed also in isolated epithelial cells of Hnf-4α KO mouse jejunum compared with control mouse jejunum, after 5 min of incubation with radiolabeled micelles (13.10 ± 4.30 vs. 22.55 ± 4.05 nmol [^{14}C]OA/mg of proteins; $P < 0.05$) (Fig. 4*C*). Finally, after 2 days of high-fat diet, higher levels of FFA, DG, and TG were recovered in the feces of KO mice compared with the control mice (TG: 2.41 ± 0.42 vs. 1.96 ± 0.36 µmol·mg feces^{-1}·g food^{-1}·24 h^{-1}; $P < 0.05$; DG: 4.71 ± 0.3 vs. 2.83 ± 0.23 µmol·mg feces^{-1}·g food^{-1}·24 h^{-1}; $P < 0.001$; FFA: 40.13 ± 2.2 vs. 32.82 ± 2.28 µmol·mg feces^{-1}·g food^{-1}·24 h^{-1}; $P < 0.001$) (Fig. 4*D*), while weight and food consumption were similar in the two groups of mice (data not shown).

The expression of FATP4 and ACS activity are reduced in Hnf-4α$^{int\Delta}$ mice. We thus analyzed the expression of proteins involved in fatty acid transport. CD36, FABPpm, and FATP4 (also named solute carrier transporter slc27a4) mRNA levels were quantified from the beginning of jejunum (I1) to the end of ileum (I3). No difference was observed for FABPpm mRNA expression (Fig. 5*A*). CD36 mRNA levels decreased from I1 to I3 segments but were found similar in both groups of mice in each intestinal fragment (Fig. 5*A*). By contrast, the levels of FATP4 mRNA differed significantly all along the intestinal tract between control (3.43 ± 0.47 in I1, 3.0 ± 0.05 in I2, 2.6 ± 0.2 in I3) and Hnf-4α$^{int\Delta}$ mice (1.6 ± 0.1 in I1, 1.8 ± 0.1 in I2, 1.48 ± 0.15 in I3). CD36 and FATP4 expression were analyzed further, through the quantification of their protein content in control and KO mice and the study of their subcellular localization. The CD36 protein level, which decreased from I1 to I3 fragment, as expected, was found unchanged between control and KO mice in each intestinal segment (Fig. 5*B*, *left* and *middle*). Immunofluorescence analysis showed that the intensity of CD36 staining was equivalent in control and KO mice, and that CD36 was essentially concentrated at the apical surface of epithelial cells, in both cases, 4 h after food withdrawal, as already reported in fasted mice (46) (Fig. 5*B*, *right*). By contrast, the FATP4 protein levels, which regularly decreased from I1 to I3 in Hnf-4α$^{loxP/loxP}$ mice (2.07 ± 0.05 in I1, 1.70 ± 0.04 in I2, 1.48 ± 0.06 in I3), were found significantly lower in the three intestinal fragments of KO mice (1.1 ± 0.03 in I1, 1.07 ± 0.03 in I2, 1.04 ± 0.04 in I3) (Fig. 5*C*, *left* and *middle*). Accordingly, immunofluorescence analysis revealed that the FATP4 signal, which exhibited the same

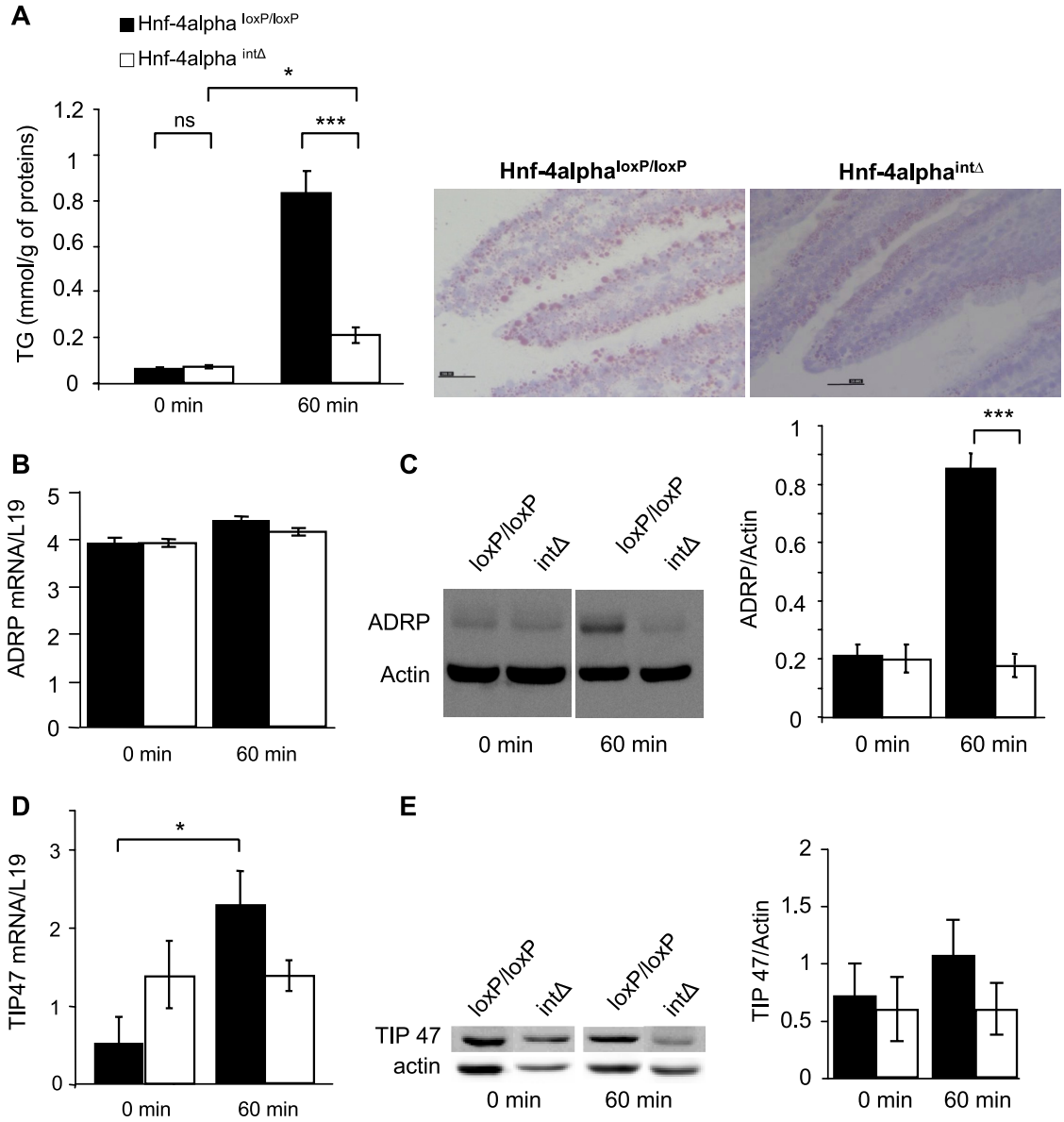

Fig. 3. *A*: the amount of TG stored in epithelial cells was analyzed 4 h after food withdrawal (0 min) and 1 h after the lipid bolus in mice treated with tyloxapol. TG were quantified in isolated epithelial cells (*left*; $n = 4$ for each group of mice and each time point) or stained with Oil red O in jejunum sections (*right*; 1 h after the lipid bolus; bar = 20 μm). Note that the global architecture of the villi is well conserved in Hnf-4α$^{int\Delta}$ mice. *B* and *D*: adipose differentiation-related protein (ADRP; *B*) and tail-interacting protein 47 (TIP47; *D*) mRNA levels were analyzed 4 h after food withdrawal (0 min) and 1 h after the lipid bolus and normalized by the corresponding levels of L19 mRNA. ADRP (*C*) and TIP47 (*E*) protein amounts were analyzed by Western blot (*left*, representative Western blots) and normalized by the signal obtained for actin (*right*). Values are means ± SE; $n = 4$ for each group of mice. $^*P < 0.05$, $^{***}P < 0.001$.

intracellular localization in both groups of mice, was greatly decreased in the intestinal epithelial cells of KO mouse jejunum (Fig. 5*C*, *right*). Finally, no significant difference was observed between control and KO mice in the protein levels of the intracellular transporters I- and L-FABP, before or 1 h after the lipid bolus (Fig. 5, *D* and *E*).

FATP4 was reported to exhibit also an ACS activity for long- and very-long-chain fatty acids. ACS activity was measured and was significantly lower in Hnf-4α$^{int\Delta}$ mice than in control mice when using OA (C18:1) (V0 = 3.03 ± 0.09 vs. 4.20 ± 0.16 μmol·min^{-1}·mg protein^{-1}; $P < 0.03$) (Fig. 6*A*) or hexacosanoic acid (C26:0) (V0 = 5.25 ± 0.6 vs. 8.5 ± 0.9 μmol·min^{-1}·mg protein^{-1}; $P < 0.05$) as substrate (Fig. 6*B*). In intestinal epithelium, long-chain ACS 1, 3, and 5 may also exert ACS activity. Their mRNA levels were analyzed and were found similar in Hnf-4α$^{int\Delta}$ mice compared with control mice (Fig. 6*C*), suggesting that the decreased ACS activity in the intestinal epithelium of Hnf-4α$^{int\Delta}$ mice might be due to the downregulation of FATP4 expression.

DISCUSSION

The increasing incidence of metabolic syndrome, the hallmarks of which include hyperglycemia, hyperlipidemia, insulin resistance, and obesity, is widely thought to result from an imbalance between increased food consumption and decreased energy expenditure. In this context, efforts are made to identify potential intestinal targets for the development of drugs reduc-

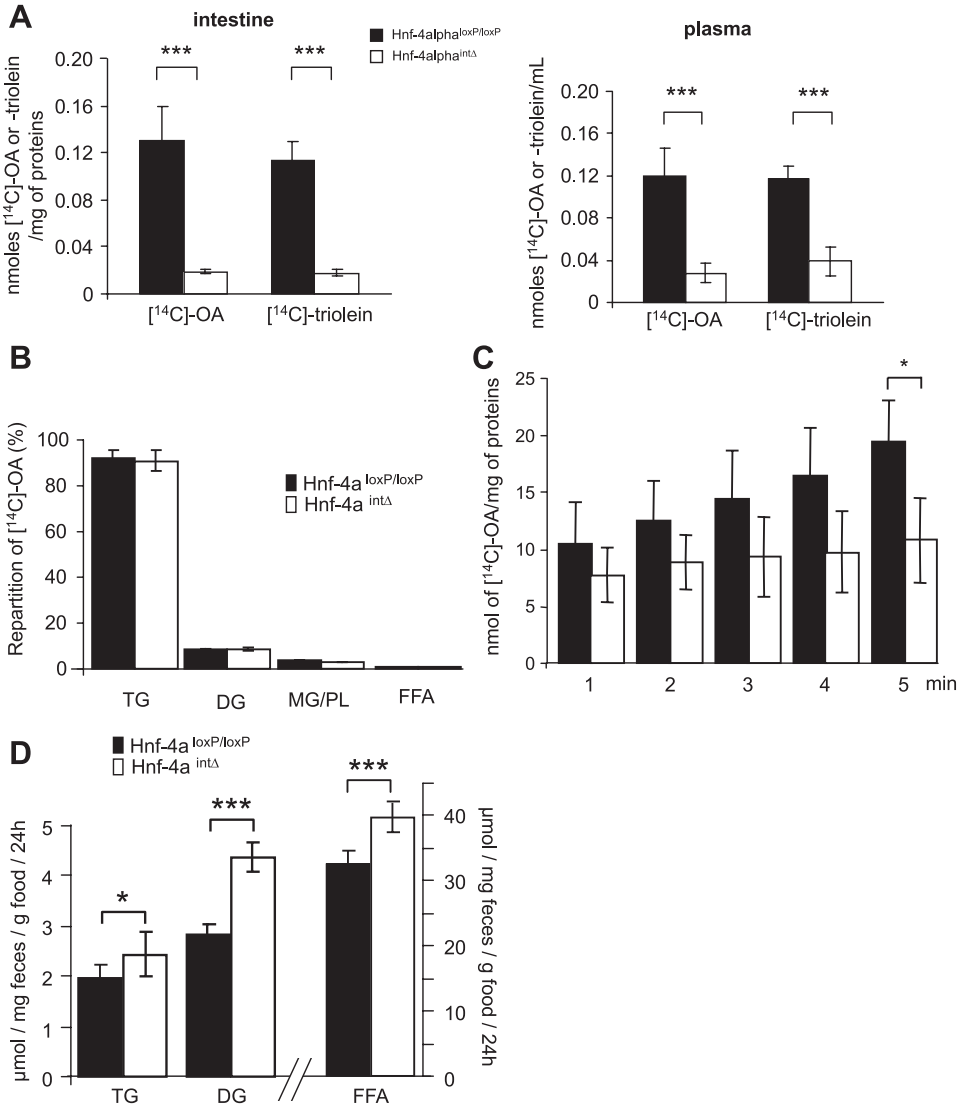

Fig. 4. *A*: 1 h after a lipid bolus containing radiolabeled oleic acid (OA) or triolein, radioactivity recovered in intestinal epithelial cells (*left*) and plasma (*right*) was quantified (solid bars, Hnf-4α$^{loxP/loxP}$ mice, $n = 4$; open bars, Hnf-4α$^{int\Delta}$ mice, $n = 4$). *B*: the repartition of labeling in epithelial cells within free fatty acids (FFA), monoglycerides/phospholipids (MG/PL), diglycerides (DG), and TG was quantified after thin-layer chromatography (solid bars, Hnf-4α$^{loxP/loxP}$ mice, $n = 3$; open bars, Hnf-4α$^{int\Delta}$ mice, $n = 5$). *C*: uptake of radiolabeled OA was measured in epithelial cells isolated freshly from jejunum of Hnf-4α$^{loxP/loxP}$ (solid bars) or Hnf-4α$^{int\Delta}$ (open bars) mice ($n = 4$ for each group of mice). *D*: the amounts of TG, DG, and FFA were quantified in feces of Hnf-4α$^{loxP/loxP}$ (solid bars) or Hnf-4α$^{int\Delta}$ (open bars) mice after 2 days of a high-fat diet ($n = 4$ for each group of mice). Values are means ± SE. $^*P < 0.05$, $^{***}P < 0.001$.

ing the risk of lipid-associated disorders and their resulting metabolic and cardiovascular diseases. In the present study, we demonstrate that HNF-4α is a key factor of the intestinal absorption of dietary lipids.

The intestinal KO of Hnf-4α gene resulted in a net decrease of the TG amounts that were secreted in plasma (Figs. 1 and 2) or present in enterocytes (Fig. 3) after a lipid bolus. These effects were due to an impairment of the uptake of fatty acids (Fig. 4). This was not a consequence of a decreased luminal TG hydrolysis, as assessed by the similar results obtained after gavage with labeled triolein or OA (Fig. 4), but was associated with lower levels of FATP4 mRNA and protein along the intestinal tract (Fig. 5) and with a lower ACS activity in Hnf-4α$^{int\Delta}$ mice compared with the control mice (Fig. 6).

The molecular mechanisms underlying long-chain fatty acid uptake are still under debate (for reviews, Refs. 19, 29). It appears now clearly that both passive diffusion and carrier-mediated mechanisms coexist. Several proteins have been shown to participate in intestinal fatty acid transport (13, 30, 43). Our results demonstrated a decreased expression of FATP4 all along the intestinal tract without alteration of FAT/CD36 expression, suggesting that the reduction of FATP4 protein amount could be involved in the lower efficiency of fatty acid uptake in Hnf-4α$^{int\Delta}$ mice. FATPs form a family of several (6 in human and 5 in mouse) related proteins that are highly conserved during evolution. The role of FATP4 as a FATP is a subject of debate. While initial studies showed significant amounts of FATP4 protein on the plasma membrane of intestinal cells (43), a recent study found that FATP4 was exclusively intracellular in intestinal epithelial cells (26). Using in vitro antisense experiments, Stahl and colleagues (43) demonstrated that FATP4 is required for fatty acid uptake into intestinal epithelial cells. Nevertheless, deletion of both FATP4 alleles resulted in embryonic lethality, and deletion of one allele of FATP4 resulted in 40% reduction of fatty acid uptake by isolated enterocytes, but did not cause any detectable effect on fat absorption in vivo (13). Recently, it was demonstrated that intestinal FATP4-deficient mice, rescued by expressing FATP4 under the control of a keratinocyte-specific promoter, did not display impairment of fatty acid uptake and of intestinal TG secretion, suggesting that FATP4 is dispensable for intestinal lipid absorption (41). Further studies are needed to better

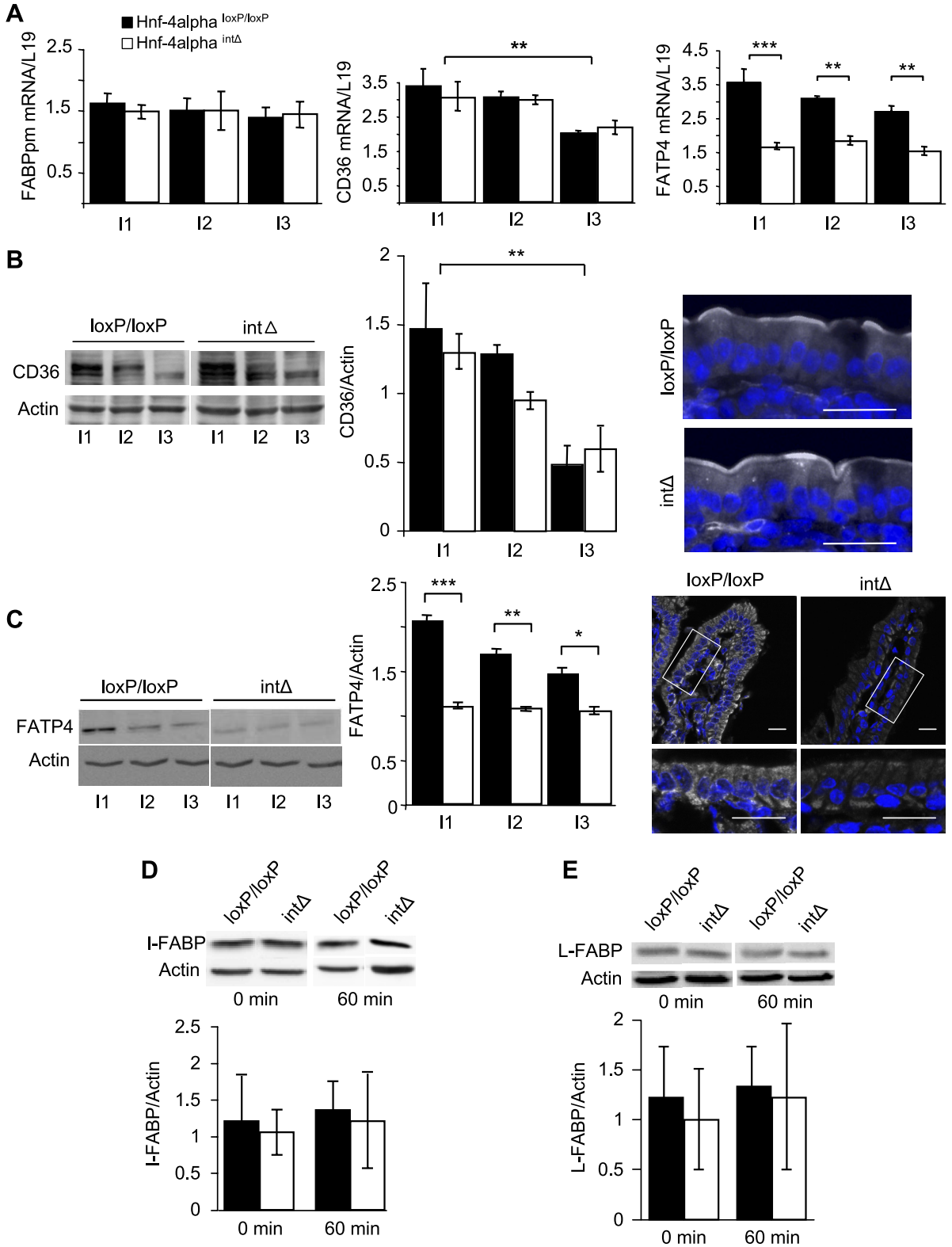

Fig. 5. *A*: fatty acid-binding protein (FABP) from the plasma membrane (FABPpm), CD36, and fatty acid transport protein-4 (FATP4) mRNA levels were analyzed in the three segments, I1 (jejunum), I2 (jejunum + ileum), and I3 (ileum), of intestine and normalized by L19 mRNA levels. CD36 (*B*) and FATP4 (*C*) protein levels were analyzed in I1, I2, and I3 by Western blots (*left* panels show representative Western blots) and normalized by the signal corresponding to actin (*middle*). Subcellular localization of CD36 (*B*) and FATP4 (*C*) was analyzed by immunofluorescence in jejunum sections of control and knockout mice (*right*; CD36 or FATP4 signal appears in white and nucleus staining in blue). For FATP4, a global picture of a villus is shown in the *top* panels, and an enlargement of the field delineated by a white rectangle in the *bottom* panels. Bar = 20 μm. I-FABP (*D*) and L-FABP (*E*) protein levels were analyzed in jejunum segments by Western blots (*top*, representative Western blots) before (0 min) and 1 h after the lipid bolus (60 min) and normalized by the signal corresponding to actin. In each experiment, $n = 6$ for each group of mice. Values are means ± SE. $^{*}P < 0.05$, $^{**}P < 0.01$, $^{***}P < 0.001$.

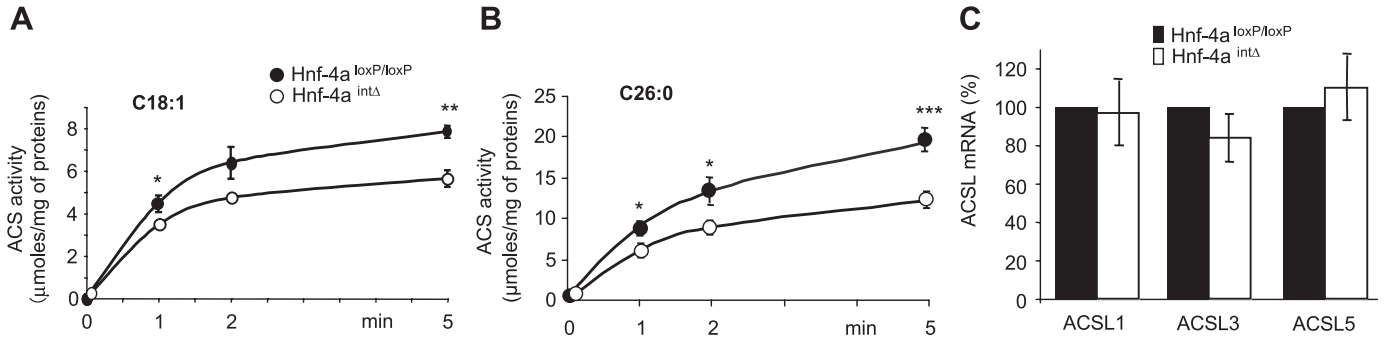

Fig. 6. Acyl-CoA synthetase (ACS) activity was measured over 5 min with epithelial cells (50 μg of proteins) isolated from jejunum fragments and using OA (C18:1; *A*) or hexacosanoic acid (C26:0; *B*) as substrate (●, Hnf-4α$^{loxP/loxP}$ mice; ○, Hnf-4α$^{int\Delta}$ mice, $n = 3$ for each point of the curves). V0 corresponds to the slope of the linear initial part of the curves. *$P < 0.05$, **$P < 0.01$, ***$P < 0.001$. *C*: long-chain ACS (ACSL) 1, 3, and 5 mRNA levels were analyzed. Percentage of mRNA levels in Hnf-4α$^{int\Delta}$ mice compared with Hnf-4α$^{loxP/loxP}$ mice are reported, with values obtained for the control mice being set at 100%. All analyses were performed 1 h after the lipid bolus in mice treated with tyloxapol (solid bars, Hnf-4α$^{loxP/loxP}$ mice; open bars, Hnf-4α$^{int\Delta}$ mice, $n = 4$ for each group of mice in each experiment). Values are means ± SE.

understand the role of FATP4 in intestinal fatty acid transport, but the constitutive deletion of FATP4 is probably not the adequate mouse model to study the importance of FATP4, because mechanisms of compensation should have occurred in intestine in this condition. FATP4 was shown to exert a fatty ACS activity, with affinity for long- and very-long-chain fatty acids (16). Supporting the relevance of this activity for a process known as "vectorial acylation", i.e., the obligatory step of acyl-CoA formation for fatty acid transport across the plasma membrane, from intestinal lumen toward enterocytes, overexpression of FATP4 in COS cells enhanced the oleate uptake while the expression of a FATP4 mutant lacking ACS activity abolished this process (26). Finally, a recent report demonstrated that FATP4 plays a role in fatty acid uptake through its intrinsic intracellular enzymatic activity (9). In Hnf-4α$^{int\Delta}$ mice, we may suggest that a decreased ACS activity governs the reduction of fatty acid uptake. The lower ACS activity observed in the intestinal epithelium of these mice may be attributed to the impaired expression of FATP4, with the expression of the other potential ACSL (ACSL 1, 3, and 5), which display a lower affinity for long- and very-long-chain fatty acids, remaining unchanged (Fig. 6). The mechanisms responsible for the activation of FATP4 promoter are still poorly known, and those through which HNF-4α may increase FATP4 expression have to be deciphered. Some authors reported an activating effect of peroxisome proliferator-activated receptor-γ on placental FATP4 expression, but the underlying mechanisms were not analyzed (38, 50). Concerning HNF-4α, the absence of consensus sequence for its direct binding to the 3.3-kb upstream from the FATP4 gene (analyzed by a web tool for predicting transcription factor binding sites, www.cbil.upenn.edu/cgi-bin/tess/tess) indicates that the effect on FATP4 expression is most probably indirect, through another HNF-4α-dependent transcription factor or via metabolic effects or via HNF-4α target genes involved in the control of mRNA stability.

HNF-4 is a member of the large family of nuclear receptors. Two genes, coding for two different isoforms, have been identified in mammals, namely Hnf-4α and Hnf-4γ. HNF-4α is expressed in the liver, but also in intestine, kidney, and pancreas, with HNF-4γ being expressed in the same tissues but not in the liver (10, 27, 35, 42, 45). HNF-4α, which is the most studied isoform, was analyzed particularly in liver and pancreas, in which it was suggested to represent a master-regulating factor of transcription (33). Using a mouse model of conditional liver-specific Hnf-4α KO, Hayhurst et al. (17) demonstrated that HNF-4α was essential to the maintenance of hepatocyte differentiation and was a major regulator of genes involved in the control of lipid homeostasis. Our present results demonstrate that the intestine-specific Hnf-4α KO induces similar but also particular effects in intestinal epithelial cells compared with hepatocytes. Indeed, mice lacking hepatic HNF-4α accumulated lipid in the liver and exhibited reduced plasma TG levels that authors explained by a decreased expression of genes encoding apoB and MTP, which are known HNF-4α targets. Postprandial TG plasma levels and intestinal apoB48 and MTP amounts were lowered also in Hnf-4α$^{int\Delta}$ mice (Figs. 1 and 2), but without accumulation of TG in enterocytes (Fig. 3). These results were due to the net decrease of fatty acid uptake, which occurred specifically in these mice (Fig. 4). Finally, while mice lacking hepatic HNF-4α expression exhibited greatly reduced plasma cholesterol and increased plasma bile acid concentrations that were attributed to a decrease in bile acid liver uptake, we did not detect changes in the plasma levels of cholesterol (Fig. 3) in Hnf-4α$^{int\Delta}$ mice.

Among metabolic diseases that are reported as linked to an impairment of HNF-4α expression is maturity onset diabetes of the young (MODY) 1 (49). Low plasma TG levels were reported in MODY1 patients (23, 25, 34, 40). In these studies, which essentially focused on the expression of liver genes, these decreased TG levels were attributed to the reduction of apoAII and CIII expression that could lead to an increased activity of lipoprotein lipase in these patients. No attention was paid to potential intestinal dysfunctions, such as a decreased fatty acid uptake, that we demonstrate to be potentially crucial.

Our present results show that HNF-4α plays important and specific roles in the process of intestinal dietary lipid absorption. More generally, they highlight that the intestinal contribution must be taken into account, along with that of other key organs, in the analysis of the mechanisms underlying phenotypic traits of metabolic diseases.

GRANTS

This work was supported by Institut National de la Santé et de la Recherche Médicale, Université Pierre et Marie Curie, and Université René Descartes.

DISCLOSURES

No conflicts of interest, financial or otherwise, are declared by the author(s).

AUTHOR CONTRIBUTIONS

V.F., M.A., A.-L.C., V.C., A.H., F.B., S.S.-J., A.R., M.L., P.C., M.R., and J.-M.L. performed experiments; V.F., M.A., A.-L.C., V.C., A.H., F.B., L.B., S.S.-J., A.R., M.L., P.C., M.R., and J.-M.L. analyzed data; V.F., M.A., A.-L.C., V.C., F.B., L.B., A.R., M.L., P.C., M.R., and J.-M.L. interpreted results of experiments; V.F., M.A., V.C., P.C., M.R., and J.-M.L. prepared figures; V.F., M.A., V.C., P.C., M.R., and J.-M.L. drafted manuscript; V.F., M.A., V.C., P.C., M.R., and J.-M.L. edited and revised manuscript; V.F., M.A., A.-L.C., V.C., A.H., F.B., L.B., S.S.-J., A.R., M.L., P.C., J.C., M.R., and J.-M.L. approved final version of manuscript; J.C., M.R., and J.-M.L. conception and design of research.

REFERENCES

1. **Archer A, Sauvaget D, Chauffeton V, Bouchet PE, Chambaz J, Pincon-Raymond M, Cardot P, Ribeiro A, Lacasa M.** Intestinal apolipoprotein A-IV gene transcription is controlled by two hormone-responsive elements: a role for hepatic nuclear factor-4 isoforms. *Mol Endocrinol* 19: 2320–2334, 2005.
2. **Bansal S, Buring JE, Rifai N, Mora S, Sacks FM, Ridker PM.** Fasting compared with nonfasting triglycerides and risk of cardiovascular events in women. *JAMA* 298: 309–316, 2007.
3. **Beaslas O, Torreilles F, Casellas P, Simon D, Fabre G, Lacasa M, Delers F, Chambaz J, Rousset M, Carriere V.** Transcriptome response of enterocytes to dietary lipids: impact on cell architecture, signaling, and metabolism genes. *Am J Physiol Gastrointest Liver Physiol* 295: G942–G952, 2008.
4. **Boquist S, Ruotolo G, Tang R, Bjorkegren J, Bond MG, de Faire U, Karpe F, Hamsten A.** Alimentary lipemia, postprandial triglyceride-rich lipoproteins, and common carotid intima-media thickness in healthy, middle-aged men. *Circulation* 100: 723–728, 1999.
5. **Borensztajn J, Rone MS, Kotlar TJ.** The inhibition in vivo of lipoprotein lipase (clearing-factor lipase) activity by triton WR-1339. *Biochem J* 156: 539–543, 1976.
6. **Carriere V, Vidal R, Lazou K, Lacasa M, Delers F, Ribeiro A, Rousset M, Chambaz J, Lacorte JM.** HNF-4-dependent induction of apolipoprotein A-IV gene transcription by an apical supply of lipid micelles in intestinal cells. *J Biol Chem* 280: 5406–5413, 2005.
7. **Cattin AL, Le Beyec J, Barreau F, Saint-Just S, Houllier A, Gonzalez FJ, Robine S, Pincon-Raymond M, Cardot P, Lacasa M, Ribeiro A.** Hepatocyte nuclear factor 4alpha, a key factor for homeostasis, cell architecture, and barrier function of the adult intestinal epithelium. *Mol Cell Biol* 29: 6294–6308, 2009.
8. **Davidson NO, Shelness GS.** Apolipoprotein B: mRNA editing, lipoprotein assembly, and presecretory degradation. *Annu Rev Nutr* 20: 169–193, 2000.
9. **Digel M, Staffer S, Ehehalt F, Stremmel W, Ehehalt R, Fullekrug J.** FATP4 contributes as an enzyme to the basal and insulin-mediated fatty acid uptake of CC muscle cells. *Am J Physiol Endocrinol Metab* 301: E785–E796, 2011.
10. **Drewes T, Senkel S, Holewa B, Ryffel GU.** Human hepatocyte nuclear factor 4 isoforms are encoded by distinct and differentially expressed genes. *Mol Cell Biol* 16: 925–931, 1996.
11. **el Marjou F, Janssen KP, Chang BH, Li M, Hindie V, Chan L, Louvard D, Chambon P, Metzger D, Robine S.** Tissue-specific and inducible Cre-mediated recombination in the gut epithelium. *Genesis* 39: 186–193, 2004.
12. **Elisaf MS, Nakou K, Liamis G, Pavlidis NA.** Tamoxifen-induced severe hypertriglyceridemia and pancreatitis. *Ann Oncol* 11: 1067–1069, 2000.
13. **Gimeno RE, Hirsch DJ, Punreddy S, Sun Y, Ortegon AM, Wu H, Daniels T, Stricker-Krongrad A, Lodish HF, Stahl A.** Targeted deletion of fatty acid transport protein-4 results in early embryonic lethality. *J Biol Chem* 278: 49512–49516, 2003.
14. **Hall AM, Brunt EM, Chen Z, Viswakarma N, Reddy JK, Wolins NE, Finck BN.** Dynamic and differential regulation of proteins that coat lipid droplets in fatty liver dystrophic mice. *J Lipid Res* 51: 554–563, 2010.
15. **Hall AM, Smith AJ, Bernlohr DA.** Characterization of the Acyl-CoA synthetase activity of purified murine fatty acid transport protein 1. *J Biol Chem* 278: 43008–43013, 2003.
16. **Hall AM, Wiczer BM, Herrmann T, Stremmel W, Bernlohr DA.** Enzymatic properties of purified murine fatty acid transport protein 4 and analysis of acyl-CoA synthetase activities in tissues from FATP4 null mice. *J Biol Chem* 280: 11948–11954, 2005.
17. **Hayhurst GP, Lee YH, Lambert G, Ward JM, Gonzalez FJ.** Hepatocyte nuclear factor 4alpha (nuclear receptor 2A1) is essential for maintenance of hepatic gene expression and lipid homeostasis. *Mol Cell Biol* 21: 1393–1403, 2001.
18. **Iqbal J, Hussain MM.** Intestinal lipid absorption. *Am J Physiol Endocrinol Metab* 296: E1183–E1194, 2009.
19. **Kampf JP, Kleinfeld AM.** Is membrane transport of FFA mediated by lipid, protein, or both? An unknown protein mediates free fatty acid transport across the adipocyte plasma membrane. *Physiology (Bethesda)* 22: 7–14, 2007.
20. **Kamstrup PR, Tybjaerg-Hansen A, Steffensen R, Nordestgaard BG.** Genetically elevated lipoprotein(a) and increased risk of myocardial infarction. *JAMA* 301: 2331–2339, 2009.
21. **Kannel WB, Vasan RS.** Triglycerides as vascular risk factors: new epidemiologic insights. *Curr Opin Cardiol* 24: 345–350, 2009.
22. **Lee B, Zhu J, Wolins NE, Cheng JX, Buhman KK.** Differential association of adipophilin and TIP47 proteins with cytoplasmic lipid droplets in mouse enterocytes during dietary fat absorption. *Biochim Biophys Acta* 1791: 1173–1180, 2009.
23. **Lehto M, Bitzen PO, Isomaa B, Wipemo C, Wessman Y, Forsblom C, Tuomi T, Taskinen MR, Groop L.** Mutation in the HNF-4alpha gene affects insulin secretion and triglyceride metabolism. *Diabetes* 48: 423–425, 1999.
24. **Liu CL, Yang TL.** Sequential changes in serum triglyceride levels during adjuvant tamoxifen therapy in breast cancer patients and the effect of dose reduction. *Breast Cancer Res Treat* 79: 11–16, 2003.
25. **Malecki MT.** Genetics of type 2 diabetes mellitus. *Diabetes Res Clin Pract* 68, *Suppl* 1: S10–S21, 2005.
26. **Milger K, Herrmann T, Becker C, Gotthardt D, Zickwolf J, Ehehalt R, Watkins PA, Stremmel W, Fullekrug J.** Cellular uptake of fatty acids driven by the ER-localized acyl-CoA synthetase FATP4. *J Cell Sci* 119: 4678–4688, 2006.
27. **Miquerol L, Lopez S, Cartier N, Tulliez M, Raymondjean M, Kahn A.** Expression of the L-type pyruvate kinase gene and the hepatocyte nuclear factor 4 transcription factor in exocrine and endocrine pancreas. *J Biol Chem* 269: 8944–8951, 1994.
28. **Mu H, Hoy CE.** The digestion of dietary triacylglycerols. *Prog Lipid Res* 43: 105–133, 2004.
29. **Nassir F, Abumrad NA.** CD36 and intestinal fatty acid absorption. *Immunol Endocr Metab Agents Med Chem* 9: 3–10, 2009.
30. **Niot I, Poirier H, Tran TT, Besnard P.** Intestinal absorption of long-chain fatty acids: evidence and uncertainties. *Prog Lipid Res* 48: 101–115, 2009.
31. **Nordestgaard BG, Benn M, Schnohr P, Tybjaerg-Hansen A.** Nonfasting triglycerides and risk of myocardial infarction, ischemic heart disease, and death in men and women. *JAMA* 298: 299–308, 2007.
32. **Nordskog BK, Phan CT, Nutting DF, Tso P.** An examination of the factors affecting intestinal lymphatic transport of dietary lipids. *Adv Drug Deliv Rev* 50: 21–44, 2001.
33. **Odom DT, Zizlsperger N, Gordon DB, Bell GW, Rinaldi NJ, Murray HL, Volkert TL, Schreiber J, Rolfe PA, Gifford DK, Fraenkel E, Bell GI, Young RA.** Control of pancreas and liver gene expression by HNF transcription factors. *Science* 303: 1378–1381, 2004.
34. **Owen K, Hattersley AT.** Maturity-onset diabetes of the young: from clinical description to molecular genetic characterization. *Best Pract Res Clin Endocrinol Metab* 15: 309–323, 2001.
35. **Plengvidhya N, Antonellis A, Wogan LT, Poleev A, Borgschulze M, Warram JH, Ryffel GU, Krolewski AS, Doria A.** Hepatocyte nuclear factor-4gamma: cDNA sequence, gene organization, and mutation screening in early-onset autosomal-dominant type 2 diabetes. *Diabetes* 48: 2099–2102, 1999.
36. **Ribeiro A, Archer A, Le Beyec J, Cattin AL, Saint-Just S, Pinçon Raymond M, Chambaz J, Lacasa M, Cardot P.** Hepatic nuclear factor-4, a key transcription factor at the crossroads between architecture and function of epithelia. *Recent Pat Endocr Metab Immune Drug Discov* 1: 166–175, 2007.

37. **Robertson MD, Parkes M, Warren BF, Ferguson DJ, Jackson KG, Jewell DP, Frayn KN.** Mobilisation of enterocyte fat stores by oral glucose in humans. *Gut* 52: 834–839, 2003.
38. **Schaiff WT, Bildirici I, Cheong M, Chern PL, Nelson DM, Sadovsky Y.** Peroxisome proliferator-activated receptor-gamma and retinoid X receptor signaling regulate fatty acid uptake by primary human placental trophoblasts. *J Clin Endocrinol Metab* 90: 4267–4275, 2005.
39. **Shen H, Howles P, Tso P.** From interaction of lipidic vehicles with intestinal epithelial cell membranes to the formation and secretion of chylomicrons. *Adv Drug Deliv Rev* 50, *Suppl* 1: S103–S125, 2001.
40. **Shih DQ, Dansky HM, Fleisher M, Assmann G, Fajans SS, Stoffel M.** Genotype/phenotype relationships in HNF-4alpha/MODY1: haploinsufficiency is associated with reduced apolipoprotein (AII), apolipoprotein (CIII), lipoprotein(a), and triglyceride levels. *Diabetes* 49: 832–837, 2000.
41. **Shim J, Moulson CL, Newberry EP, Lin MH, Xie Y, Kennedy SM, Miner JH, Davidson NO.** Fatty acid transport protein 4 is dispensable for intestinal lipid absorption in mice. *J Lipid Res* 50: 491–500, 2009.
42. **Sladek FM, Zhong WM, Lai E, Darnell JE Jr.** Liver-enriched transcription factor HNF-4 is a novel member of the steroid hormone receptor superfamily. *Genes Dev* 4: 2353–2365, 1990.
43. **Stahl A, Hirsch DJ, Gimeno RE, Punreddy S, Ge P, Watson N, Patel S, Kotler M, Raimondi A, Tartaglia LA, Lodish HF.** Identification of the major intestinal fatty acid transport protein. *Mol Cell* 4: 299–308, 1999.
44. **Stegmann A, Hansen M, Wang Y, Larsen JB, Lund LR, Ritie L, Nicholson JK, Quistorff B, Simon-Assmann P, Troelsen JT, Olsen J.** Metabolome, transcriptome, and bioinformatic cis-element analyses point to HNF-4 as a central regulator of gene expression during enterocyte differentiation. *Physiol Genomics* 27: 141–155, 2006.
45. **Taraviras S, Mantamadiotis T, Dong-Si T, Mincheva A, Lichter P, Drewes T, Ryffel GU, Monaghan AP, Schutz G.** Primary structure, chromosomal mapping, expression and transcriptional activity of murine hepatocyte nuclear factor 4gamma. *Biochim Biophys Acta* 1490: 21–32, 2000.
46. **Tran TT, Poirier H, Clement L, Nassir F, Pelsers MM, Petit V, Degrace P, Monnot MC, Glatz JF, Abumrad NA, Besnard P, Niot I.** Luminal lipid regulates CD36 levels and downstream signaling to stimulate chylomicron synthesis. *J Biol Chem* 286: 25201–25210, 2011.
47. **Williams KJ.** Molecular processes that handle–and mishandle–dietary lipids. *J Clin Invest* 118: 3247–3259, 2008.
48. **Xie Y, Newberry EP, Young SG, Robine S, Hamilton RL, Wong JS, Luo J, Kennedy S, Davidson NO.** Compensatory increase in hepatic lipogenesis in mice with conditional intestine-specific Mttp deficiency. *J Biol Chem* 281: 4075–4086, 2006.
49. **Yamagata K, Furuta H, Oda N, Kaisaki PJ, Menzel S, Cox NJ, Fajans SS, Signorini S, Stoffel M, Bell GI.** Mutations in the hepatocyte nuclear factor-4alpha gene in maturity-onset diabetes of the young (MODY1). *Nature* 384: 458–460, 1996.
50. **Zhu MJ, Ma Y, Long NM, Du M, Ford SP.** Maternal obesity markedly increases placental fatty acid transporter expression and fetal blood triglycerides at midgestation in the ewe. *Am J Physiol Regul Integr Comp Physiol* 299: R1224–R1231, 2010.